



117
153
THS



This is to certify that the
thesis entitled
On Improving Ge Detector Energy Resolution
and Peak-to-Compton Ratios by
Pulse-Shape Discrimination
presented by

Nobuo Matsushita

has been accepted towards fulfillment
of the requirements for

M.S. degree in Physical Chemistry

Wm. C. M. Hamis

Major professor

Date 8 August 1980



OVERDUE FINES:

25¢ per day per item

RETURNING LIBRARY MATERIALS:

Place in book return to remove
charge from circulation records

ON IMPROVING GE DETECTOR ENERGY RESOLUTION AND
PEAK-TO-COMPTON RATIOS BY PULSE-SHAPE DISCRIMINATION

By

Nobuo Matsushita

A THESIS

Submitted to
Michigan State University
in partial fulfillment of the requirements
for the degree of

MASTER OF SCIENCE

Department of Chemistry
Program in Physical Chemistry

1980

ABSTRACT

ON IMPROVING GE DETECTOR ENERGY RESOLUTION AND
PEAK-TO-COMPTON RATIOS BY PULSE-SHAPE DISCRIMINATION

By

Nobuo Matsushita

The rise-time discrimination of pulses from Ge detectors can be used to improve the spectra on two levels: First, by discriminating against slower-rising pulses, both the energy resolution and peak-to-Compton ratios can be improved significantly, especially for detectors that have suffered neutron damage. Second, by adding a pulse-height correction to compensate for effects of varying rise-time, an improved composite spectrum can be obtained without significant loss in detector efficiency.

6116470

ACKNOWLEDGMENTS

I wish to thank Dr. Wm. C. McHarris for his encouragement and guidance during the preparation of this thesis. I would also like to thank Dr. R. B. Firestone for his valuable advice and helpful time-consuming discussions.

I also wish to extend special thanks to Drs. J. Kasagi and J. A. Nolen, Jr., for their invaluable assistance and encouragement during the data acquisition and analysis of this work. Many of their ideas led to solutions to apparently insurmountable problems.

Thanks to Mr. R. Au, Mr. W. Bentley, Mr. R. Fox and Mr. B. Jeltema for their programing help.

Ms. Rose Manlove aided greatly by typing the final version of this manuscript.

Much of the financial assistance for this research has been provided by the National Science Foundation and Michigan State University.

TABLE OF CONTENTS

	Page No.
LIST OF FIGURES.	iv-v
Chapter	
I. INTRODUCTION	1
II. TWO DIMENSIONAL EXPERIMENT	4
1. Experimental Techniques.	4
2. Results and Discussion	5
III. THREE DIMENSIONAL EXPERIMENT	17
1. Experimental Techniques and Data Processing.	20
2. Results and Discussion	22
IV. CONCLUSIONS.	31
BIBLIOGRAPHY	33
APPENDICES	
A. Event Rec.	36
B. Auto Cen	38
C. 2D GATE.	40

LIST OF FIGURES

Figure		Page No.
2-1	Block diagram of the fast-slow coincidence circuit used	6
2-2	Rise-time discriminated spectra with Ge planar detector	7
2-3	Output of the TAC for the spectra shown in fig. 2-2.	8
2-4	Summary of the analysis.	10
2-5	Plots of the centroid of four energies as a function of the pulse rise-time	12
2-6	The correlation between the rise-time and the centroid of the 1332.5-keV peak.	14
2-7	Rise-time discriminated spectrum (top) compared with a raw spectrum (bottom).	15
2-8	Blow up of a portion of fig. 2-7	16
3-1	A Coaxial Detector Structure	18
3-2	An expected correlation of the time difference between the 0.1-0.5 fraction and the 0.1-0.7 fraction	19

Figure	Page No.
3-3	The block diagram for the three parameter experiment 21
3-4	The correlation between the centroid of the 1332.5-keV peak and the two TAC signals. 23
3-5	90° clockwise rotation of fig. 3-4 24
3-6	The relative yield for each 1332.5-keV peak vs the two TAC signals. 25
3-7	90° clockwise rotation of fig. 3-6 26
3-8	The two dimensional plots displaying the gated regions for 2D GATE. 28
3-9	Spectrum with the 2D GATE (bottom) compared with the raw data (top) 29
3-10	Blow up of a portion of fig. 3-9 30

CHAPTER I

INTRODUCTION

Until semiconductor detectors were introduced in nuclear science, scintillation counters were used in nuclear spectroscopy. The use of the scintillation counter in its various forms has made possible the investigation of a large number of problems that would otherwise have been extremely tedious if not impossible. As an example we may consider the field of gamma (γ)-ray spectroscopy, whose present state of development is due in large part to the use of scintillators. Prior to about 1949, γ -ray energies were generally measured either by observing the beta spectrum of associated Compton recoils or photoelectron recoils or by interposing absorbers of various materials between the γ source and detector (Geiger counter). The development of scintillation counters, especially the NaI(Tl) detector, have provided a convenient, high-efficiency spectrometer such that measurements of γ -ray spectra from radioactive nuclei have become a fairly common laboratory technique. In the best scintillation systems one photoelectron is produced at the photocathode for each 110 eV of energy lost [Co71].

In the early 1960's, semiconductors were introduced in nuclear science. Since then, almost constant effort has been expended to improve both their energy resolution and their peak-to-Compton ratio [Ie71] to some extent, mutually incompatible goals. For example, the larger the detector, the better the peak-to-Compton ratio, but in

general, the poorer its resolution. Such panaceas as very large volume intrinsic Ge detectors [Go74] or successful fabrication of detectors from semiconductors having both a high Z and a small band gap [Pe72], (i.e., InSb) have not yet appeared on the scene. Thus, we often find a necessary compromise: a Ge γ -ray detector with the best energy resolution practicable (and often of medium to small size) used in conjunction with one of the more or less elaborate Compton-suppression spectrometers [Au67,Be77]. The latter are necessarily expensive, cumbersome, and require elaborate coincidence electronics.

Additional concern arises when Ge detectors have been used for in-beam γ -ray experiments where they often suffer from neutron damage. The neutrons can cause lattice defects in the Ge crystal which act as traps for the charge carriers [Go74,Kr68,Ma68]. These trapping centers not only contribute to poor resolution because of incomplete charge collection, but also slow down the rate of charge collection [Ma68]. Often in-beam γ -ray experiments extend over periods of days. In such cases neutron damage may be occurring continuously and the resolution will degenerate accordingly.

One way to repair these neutron damaged detectors is to regenerate the Ge crystal. One can attempt to regenerate the crystal by the Badger Method [Ba74]. This method is not always successful, so the detector is often sent back to the company.

Our original purpose was to investigate the different rise-time signals from Ge detectors, since this information might suggest some ways of improving the energy resolution of the detectors. Also, at the same time, we were interested in how the relative efficiency and the

peak-to-Compton ratios depended on the rise-times. In general, the poor energy resolution is associated with pulses having slower than normal rise-times. By discriminating against slower pulses one should be able to improve the energy resolution of a detector, albeit at some expense in efficiency.

The improvement in the energy resolution has been borne out by my experiments. I found that I can improve the energy resolution of a detector by approximately 50%, the exact amount of depending on the amount of neutron damage the detector has suffered. For a brand new, state-of-the-art, high-resolution detector, the effect is not very great; for a badly damaged detector, the improvement can exceed 50%. Unexpectedly, however, I also found that I can use pulse-height correction techniques to gain these improvements without any significant loss in efficiency.

CHAPTER II
TWO DIMENSIONAL EXPERIMENT

1. Experimental Techniques

I have performed experiments using several Ge and Ge(Li) detectors--from different manufacturers, of various sizes, and of both planar and coaxial configurations. In this thesis, however, I present results only for the two detectors studied most extensively: a Ge planar detector manufactured by Princeton Gamma-Tech and a Ge(Li) true coaxial detector manufactured by ORTEC.

The planar detector had an active area of 1000 mm^2 , giving it an active volume of 13 cm^3 , or an efficiency of 2.5% relative to a 7.6×7.6 -cm NaI(Tl) detector (for the ^{60}Co 1332.5-keV peak, with a source-to-detector distance of 25 cm). The operational bias was 2500 V, and the original energy resolution (again, for the ^{60}Co 1332.5-keV) was 1.7 keV full width at half maximum (FWHM), although the resolution had deteriorated slightly to 1.84 keV FWHM at the time these measurements were performed.

The true coaxial detector was 44.4 mm long, 49.6 mm in diameter, and with a drift depth of 19.3 mm, resulting in an active volume of 78.3 cm^3 , or an efficiency of 16%. Its operational bias was 4800 V, and its original warranted resolution was 2.0 keV FWHM. This detector, however, had been used extensively for in-beam experiments and had suffered extensive neutron damage, resulting in a poorer energy resolution of 4.92 keV.

Standard ^{60}Co , ^{137}Cs , ^{152}Eu sources were used for my measurements.

In order to perform our rise-time experiments, I used a fast-slow "megachannel" [Gi71] circuit with branched signals from the single detector under investigation for the coincidence inputs. A block diagram of the experimental set-up is shown in fig. 2-1. The ORTEC Model 473 Constant Fraction Timing Discriminators (CFTD), together with associated Model 425 Delays, were used to start and stop the Model 467 Time-to-Amplitude Converter (TAC), whose output was recorded on magnetic tape along with the pulse-height information.

Although the rise-time distributions vary from detector to detector, 40 nsec on the external delays for the CFTD's was determined to be an appropriate setting for these experiments (one has to be wary, in particular, of using much shorter delays--these can sometimes cause the CFTD's to act somewhat as lower-level discriminators for the slower-rise pulses, thus artificially eliminating some of the lower-energy events for slow rise times). The 0.1 fraction CFTD was used to start the TAC; the 0.5 fraction CFTD, to stop the TAC. Thus the rise-time is the time difference between the output of 0.1 and 0.5 fraction CFTD. All data were recorded event by event on magnetic tape and later sorted, using the II-Event [Au72] data taking and II-Event Recovery [Au75] programs on the MSU NSCL Sigma-7 computer.

2. Results and Discussion

Examples of $^{60}\text{Co} + ^{152}\text{Eu}$ spectra taken with the Ge planar detector are shown in fig. 2-2, and the output of the TAC for these spectra is shown in fig. 2-3. The "all-event" spectrum shown at the bottom of fig. 2-2 in A) was obtained by integrating over all the TAC signals.

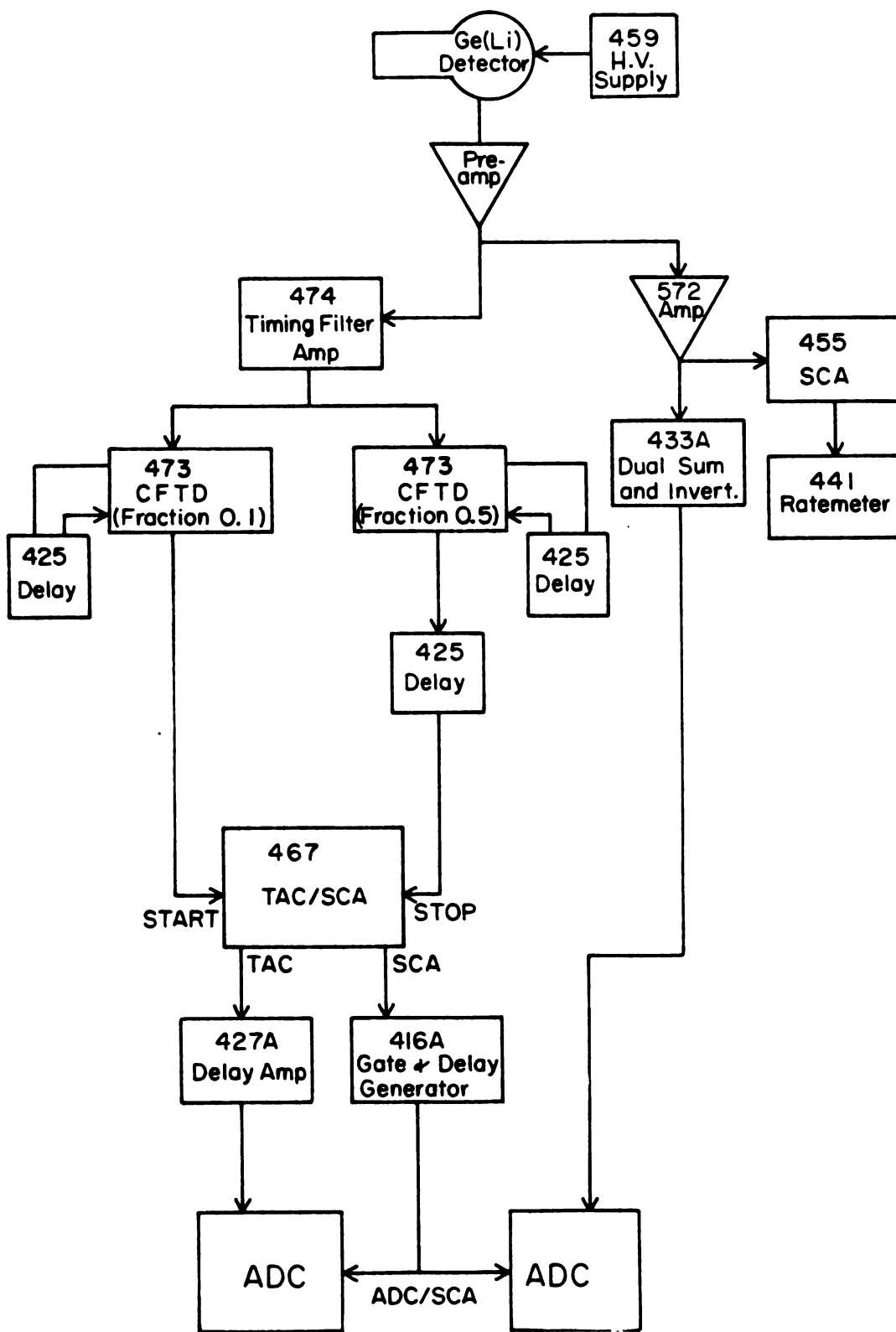


Figure 2-1

Block diagram of the fast-slow coincidence circuit used

7
Planar Detector

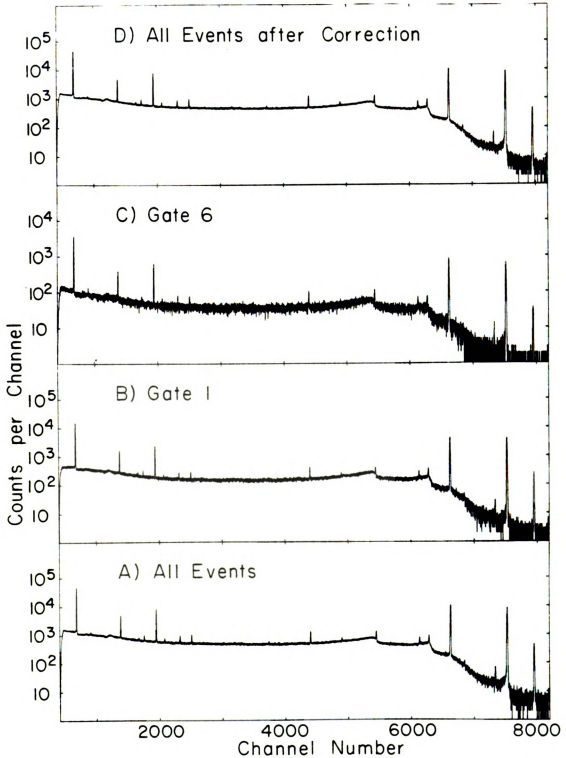


Figure 2-2

Rise-time discriminated spectra with Ge planar detector

Planar Detector TAC Spectrum

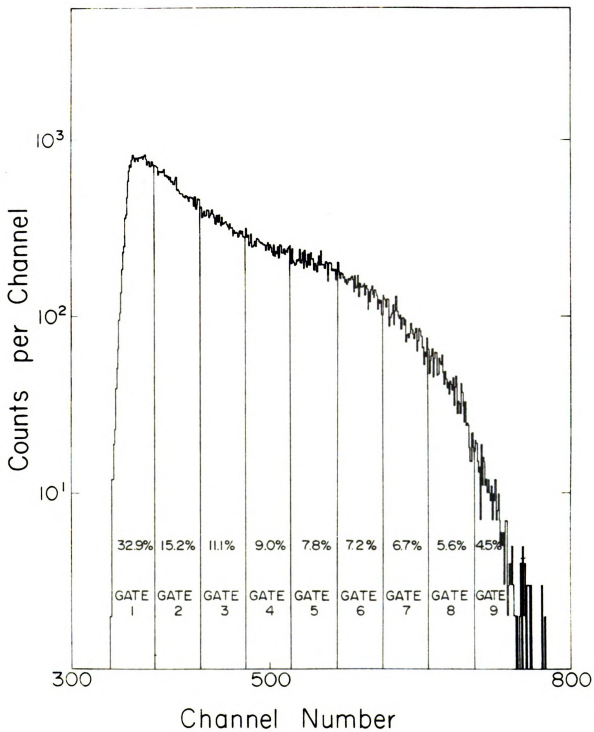


Figure 2-3

Output of the TAC for the spectra shown in fig. 2-2

Nine separate gates were taken, covering a 45-nsec range. In B) a fast rise-time spectrum is shown (Gate 1), while in C) a considerably slower one is shown (Gate 6). Finally, at the top of fig. 2-2, in D), I show an "all-events" spectrum that has been pulse-height corrected in the manner described below.

In fig. 2-4 I show a summary of my analysis of the nine TAC-gated spectra: The energy resolution versus TAC channel is shown in the middle. The resolution (for the ^{60}Co 1332.5-keV peak) has been improved by approximately 10% in the faster rise-time slices. Correspondingly, the peak-to-Compton ratio is shown as a function of rise-time, where it can be seen there is a ten-fold improvement between the poorest (Gate 9) and the best (Gate 1). At the bottom of the figure I show the fraction of total events occurring in each slice.

As anticipated, better energy resolution and peak-to-Compton ratios can be obtained by discriminating against pulses having slower rise-times, as demonstrated in fig. 2-4. Somewhat more surprising, however, is the fact that, for most of the slices, the individual energy resolution and peak-to-Compton ratios are better than in the raw "all-events" spectrum. Encouraged by this result, I made a more elaborate investigation of each peak shape and centroid position.

The lattice defects contribute to degraded resolution because they can act as traps for the charge carriers, leading to incomplete charge collection. At the same time they slow down the rate of the charge collection. It would not matter if all the charge were not collected, provided a constant percentage of the charge were collected for every event. This would change the normalization, but, in

Planar Detector (1332.5 keV)

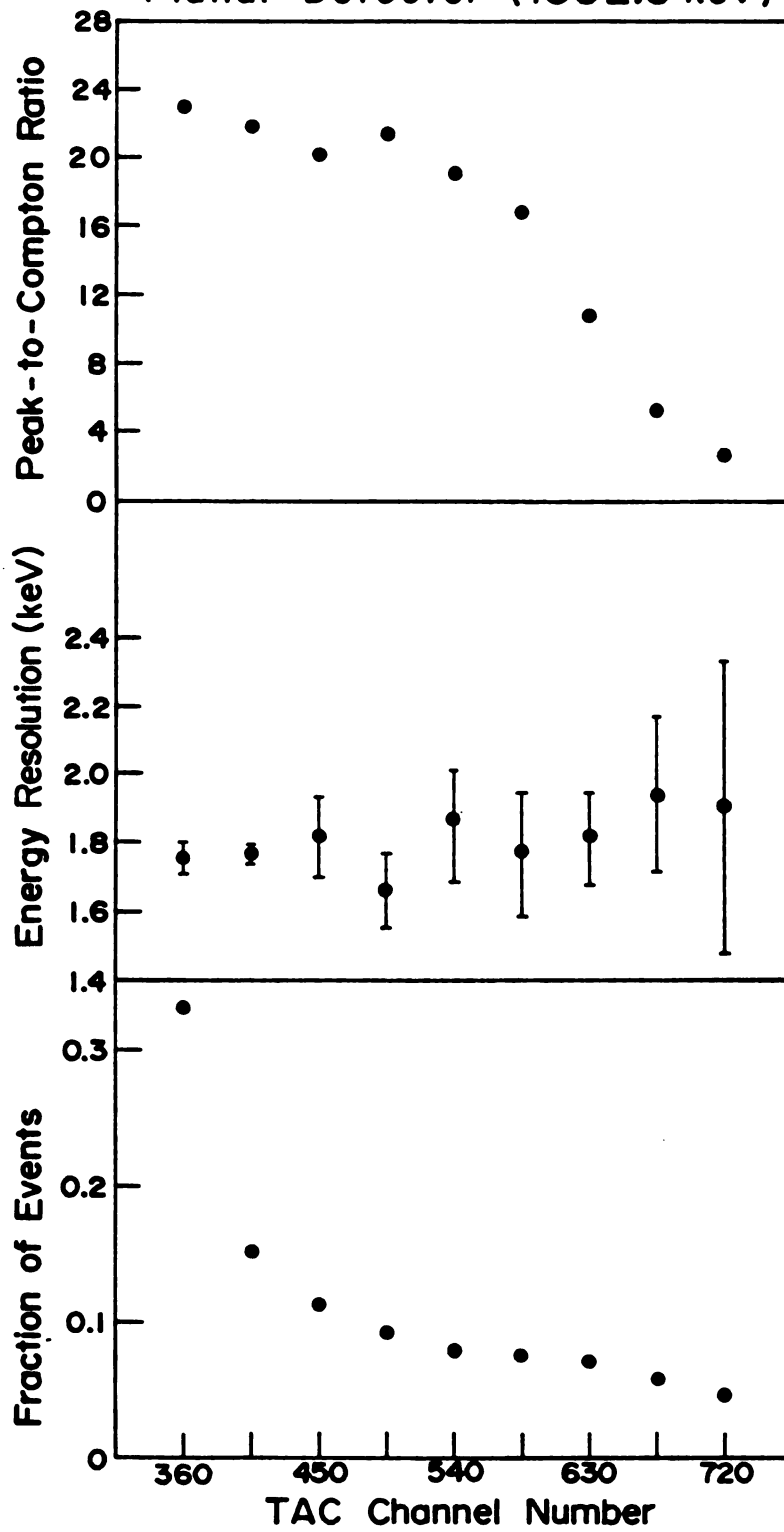


Figure 2-4

Summary of the analysis

principle, one could obtain quite good resolution in such a system even without complete charge collection. If there is a direct correlation between the rise-time of a pulse and the percent of charge collected, one has a means with which to work on the problem.

In fig. 2-5 I have plotted the centroid of four different γ -ray peaks versus the TAC channel: The peaks shift linearly as a function of the rise-time, and the slopes for the lines are energy dependent, being greater for the higher-energy peaks. The slope of the line for each peak can be fitted to relation

$$A = \alpha E \quad (1)$$

Here α is a constant and E is the energy. This indicates that the amount of charge trapped in the damaged portions of a detector is proportional to the energy.

This linear dependence makes it easy to develop computer software to shift each pulse-height value by an amount determined by the rise-time and the pulse-height. The amount of each shift is given by

$$E_{\text{shift}} = AT \quad (2)$$

After this correction, the "all-events" resolution for the 1332.5-keV ^{60}Co peak improved from 1.84 keV to 1.77 keV FWHM. This is not a remarkable improvement; however, this detector originally had quite good resolution. Had it suffered more extreme neutron damage, I assume that the improvement would have been greater. In principle, the use of more and narrower rise-time slices should make a further improvement up to the theoretical limit of time resolution.

Centroid vs TAC Gate (Planar Detector)

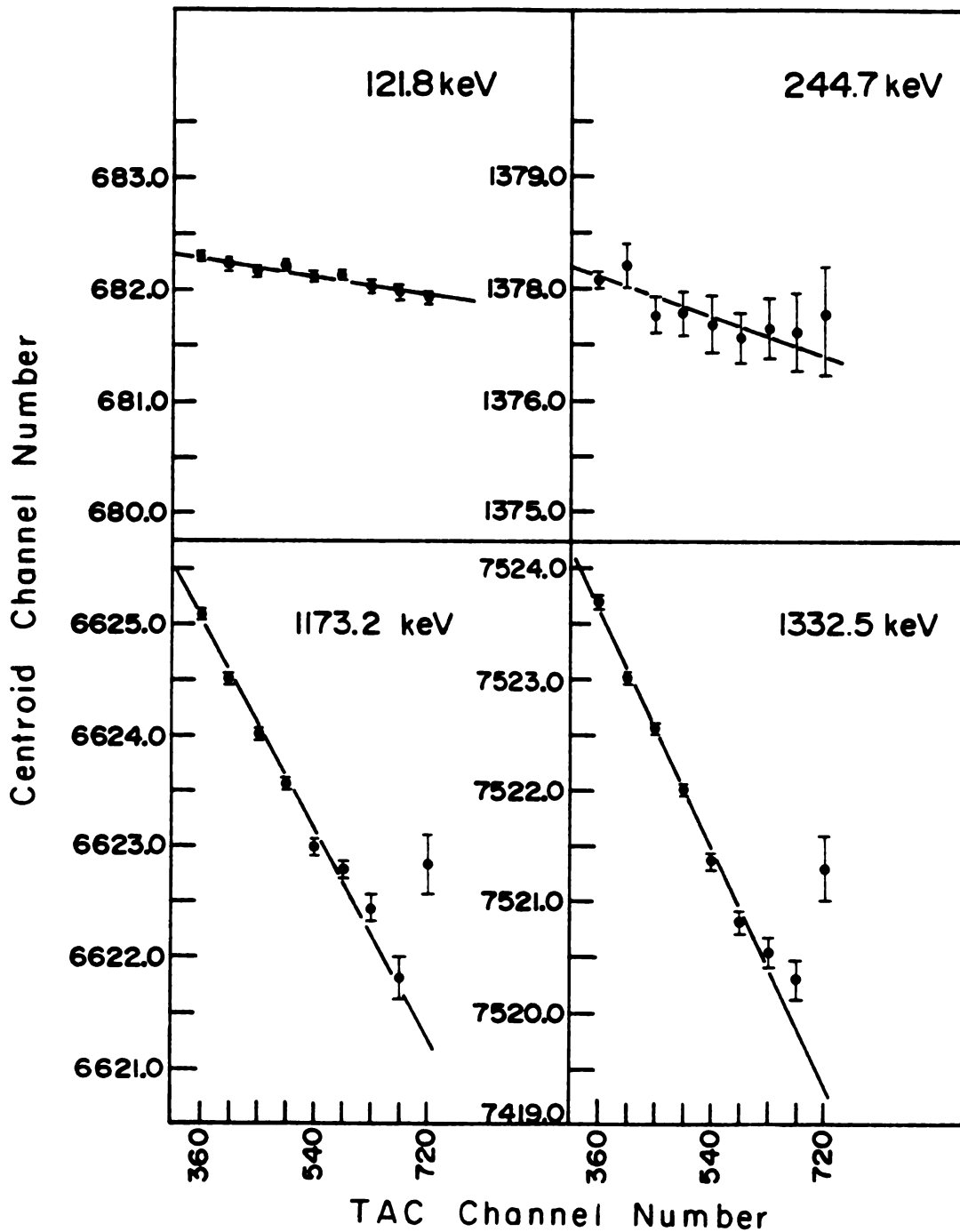


Figure 2-5

Plots of the centroid of four energies as a function of the pulse rise-time.

The same method was applied for the coaxial Ge(Li) detector which had indeed suffered considerable neutron damage. Fig. 2-6 shows the correlation between the rise-time versus the 1332.5-keV γ -ray line shape. This figure shows that with increasing rise-time (i.e., increasing the gate number), the peaks get broader and split into a doublet. This splitting phenomenon has also been seen in a previous study [Kr68].

The pulse-height correction method is only suitable if there is some relation between the pulse-height and the rise-time. The individual energy resolution of the gated spectra must be better than the raw data energy resolution. Thus, for the coaxial detector case, even if we could correct for the pulse-height, it would not be expected to improve the energy resolution. With 5% efficiency, by choosing the rise-time gate, I could get 2.31 keV FWHM (vs 4.92 keV for the raw data), or an energy resolution improvement of 53%. The "all-events" and fast rise-time spectra (corresponding approximately to Gates 1-2 in fig. 2-3) are shown in fig. 2-7. An expanded comparison of these two spectra is given in fig. 2-8, where the spectra have been normalized to the height of the 1173.2-keV peak.

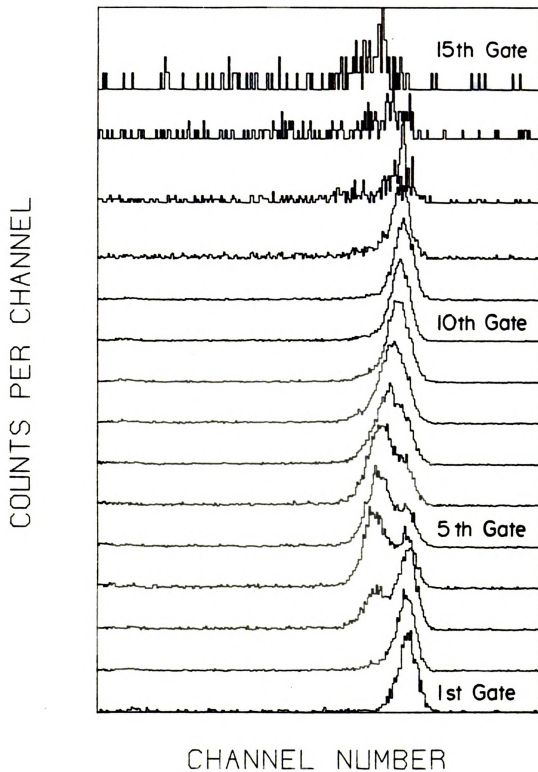
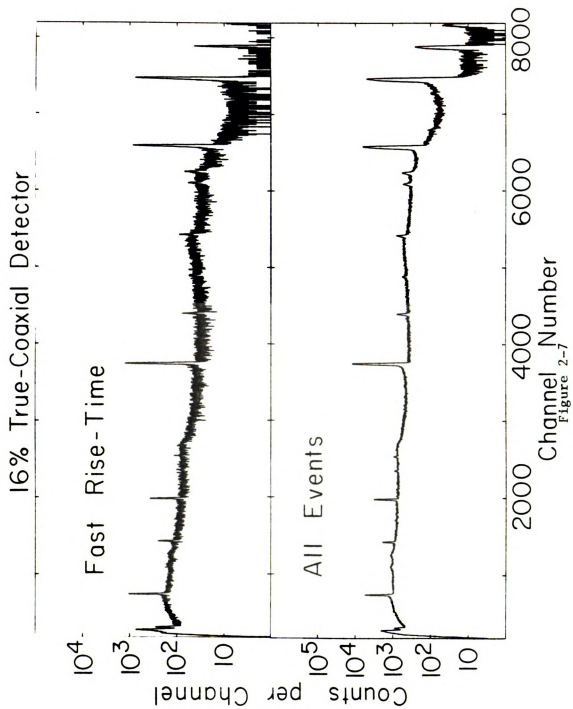
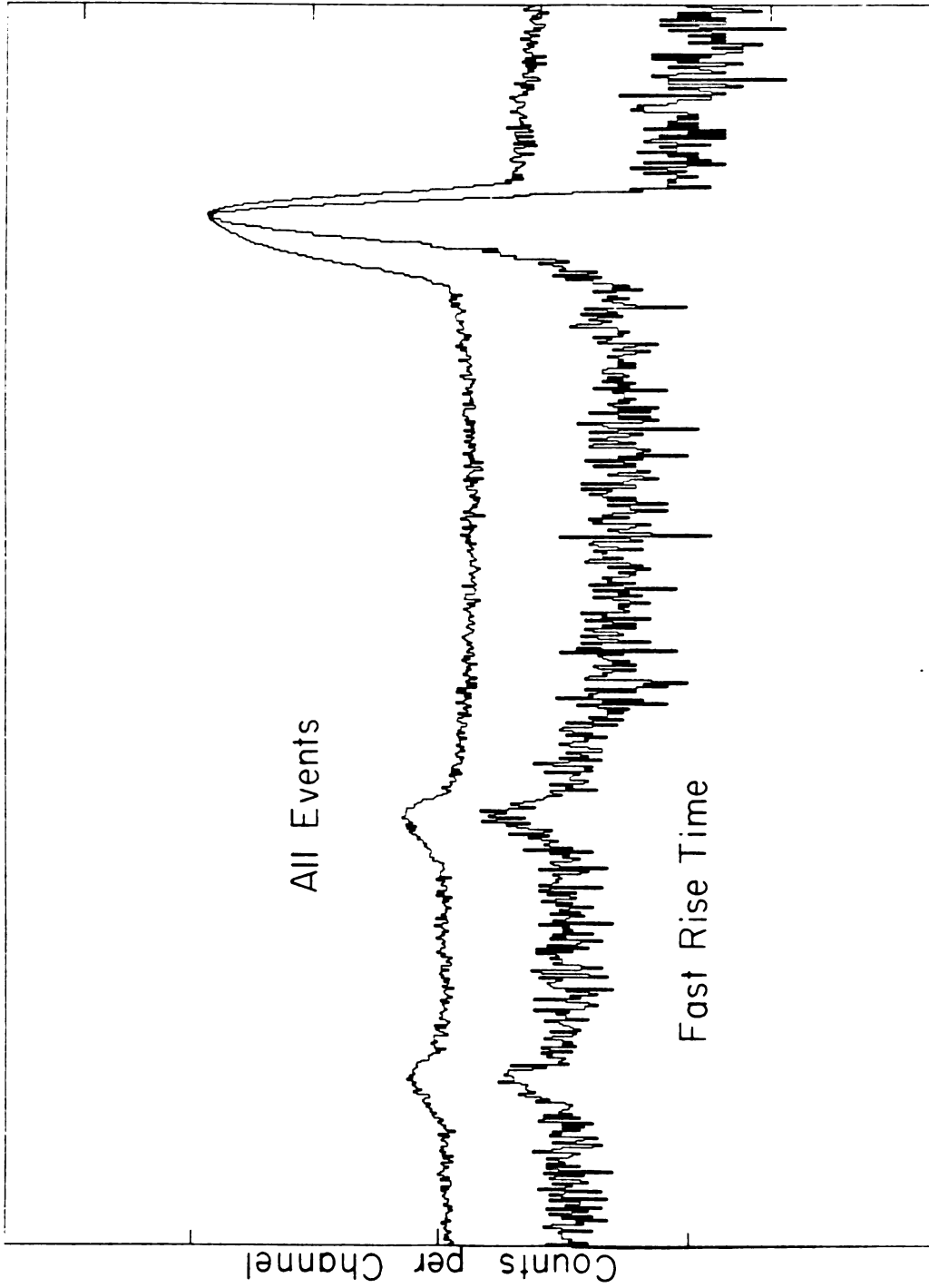


Figure 2-6

The correlation between the rise-time and the centroid of the 1332.5-keV peak.



Rise-time discriminated spectrum (top) compared with a raw spectrum (bottom)



Channel Number

Figure 2-8

Blow up of a portion of fig. 2-7

CHAPTER III

THREE DIMENSIONAL EXPERIMENT

In general, the pulse shape of a coaxial Ge(Li) detector is determined by the electric field as a function of the position inside the detector's sensitive region. The following equation gives the integrated voltage (V) for a coaxial detector as shown in fig. 3-1.

$$\begin{aligned}
 v = \frac{Q}{C} \frac{1}{\log(b/a)} & \left[\left(\log(X_o^2 + (b^2 - X_o^2) \frac{t}{T_{ion}}) - \log X_o^2 \right) \right. \\
 & \left. + \left(\log X_o^2 - \log(X_o^2 - (X_o^2 - a^2) \frac{t}{T_{el}}) \right) \right] \quad (3) \\
 & (t \leq T_{el} \text{ and/or } T_{ion})
 \end{aligned}$$

Here, T_{ion} and T_{el} are collection time for ion and electron respectively. Q is the charge, and C is the capacitance. The other terms are referred to in fig. 3-1. The pulses have different rise-times, from 60 nsec to 150 nsec, depending on the interacting positions. This creates a much more complicated relation between the pulse-height and the rise-time. For example, consider the two pulses A and B: A is a slow rise-time pulse, the slow rise-time resulting from neutron damage, and B is a naturally slow rise-time pulse without neutron damage. These pulses, A and B, arrive at the same time at the 0.5 fraction level. Since A is the neutron damaged pulse, its pulse-height is smaller than that of B.

However this complication may be solved by adding another CFTD. Fig. 3-2 shows the expected correlation of the time difference

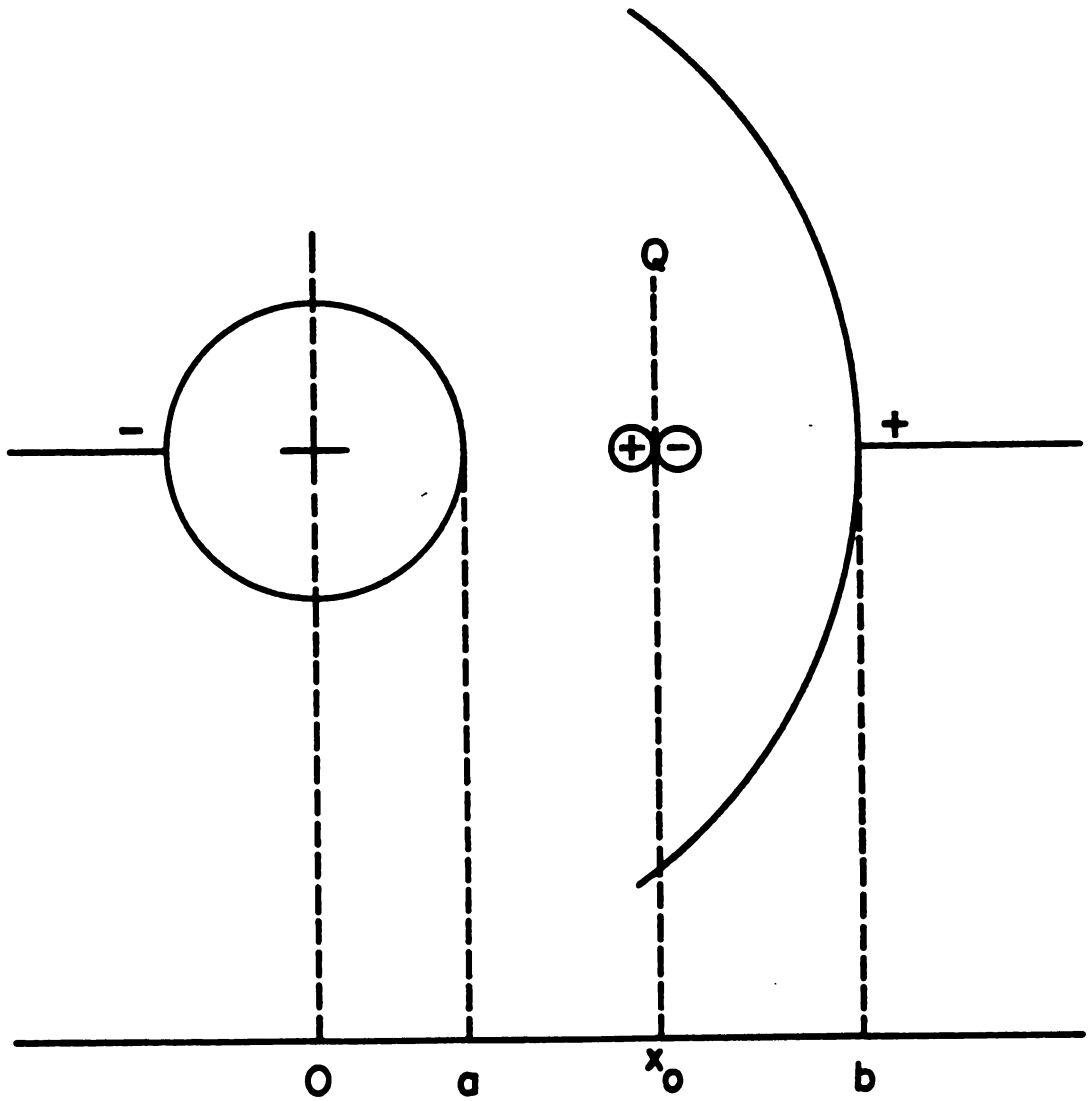


Figure 3-1

A Coaxial Detector Structure.

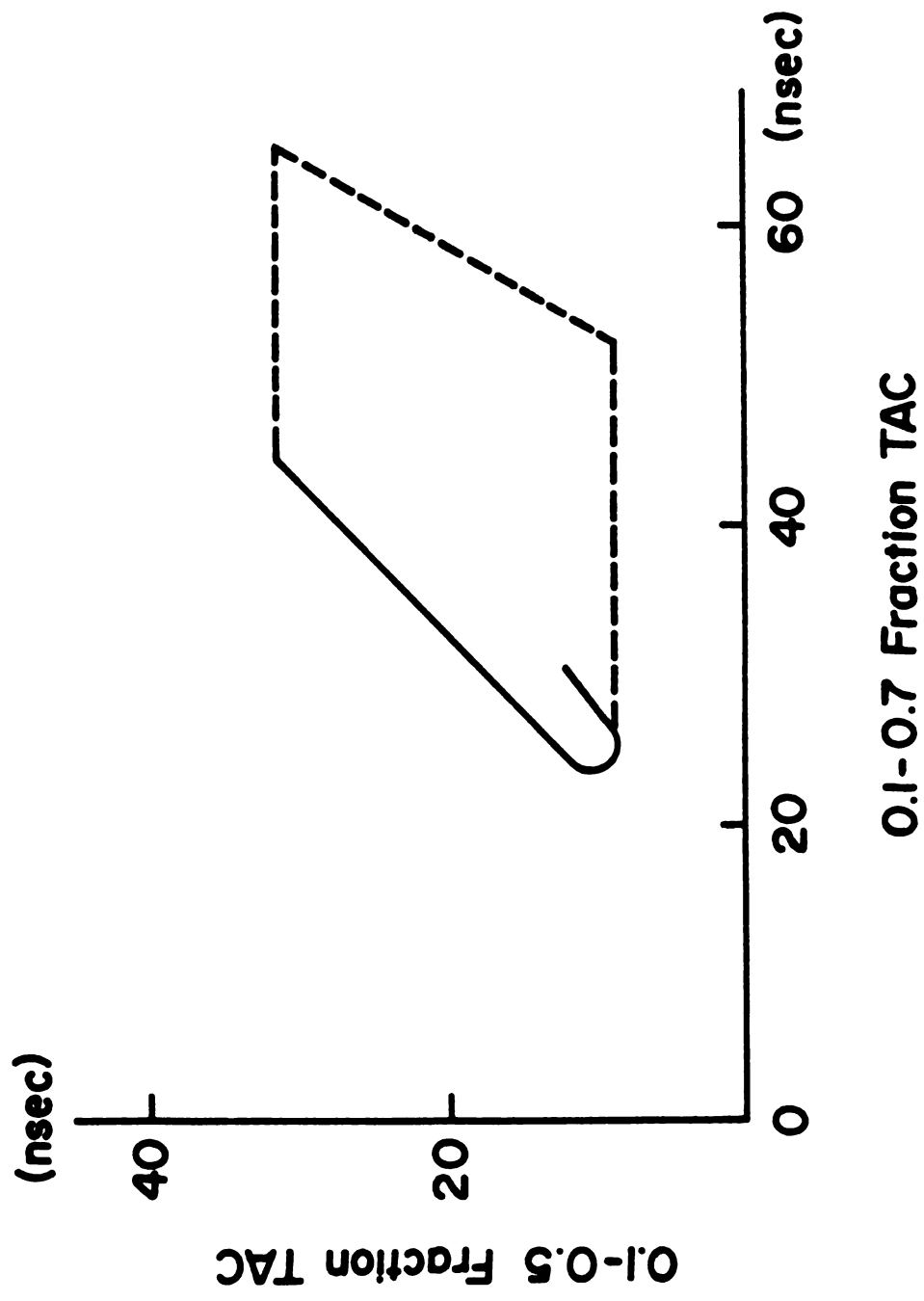


Figure 3-2
An expected correlation of the time difference
between the 0.1-0.5 fraction and the 0.1-0.7 fraction.

between the 0.1-0.5 fraction and the 0.1-0.7 fraction. The solid line indicates the calculated correlation of the output pulse from the timing filter amplifier with a shaping time constant of 50 nsec [Ka80]. For ideal conditions, we expect all events to be distributed on the line in fig. 3-2. For neutron damaged cases, I expect those linear distributions to become area distributions because it takes more time to collect pulses.

1. Experimental Techniques and Data Processing

The block diagram for the triple coincidence experimental electronics is shown in fig. 3-3. This diagram is similar to that used previously, except that there is another CFTD and TAC. The detector was the 16% Ge(Li) detector previously used, and I used the same radiation sources.

The 0.1 fraction level of the CFTD was used to start both TAC's; the 0.5 fraction and the 0.7 fraction levels were used to stop them. Therefore, for one ADC the input signal is proportional to the rise-time differences between the 0.1 and 0.7 fraction levels of the CFTD, and for the other ADC the input is the time difference between the 0.1 and the 0.5 fraction levels. All data were recorded event by event on magnetic tape using II-event program as before and sorted off-line.

In order to see the centroid movement for short calculation time, it was necessary to develop a new sorting program: Event Rec. This program allows me to accumulate the three dimensional ($20 \times 25 \times 200$ channels) energy spectrum. I used 200 channels for an energy spectrum, 25 channels for the 0.5 TAC, and 20 channels for the 0.7 TAC. Then,

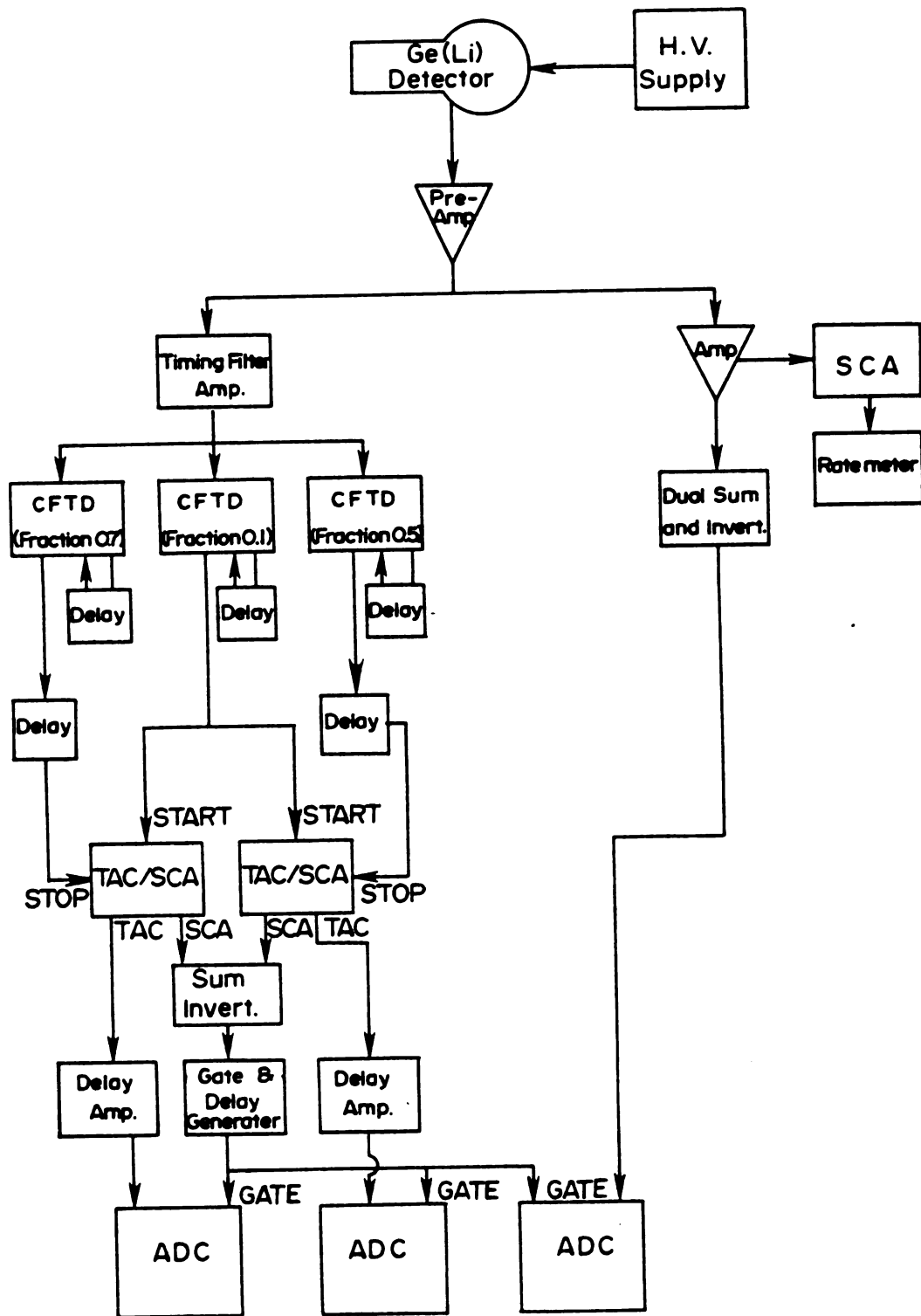


Figure 3-3

The block diagram for the three parameter experiment.

after data were sorted by Event Rec, the centroid of all 500 TAC gated spectra were obtained by a program called Auto Cen. This program outline is as follows:

1. Find the highest count channel.
2. Find the channels of the beginning and the end of the peak.
3. Calculate the centroid. The background is determined by averaging the number of counts per channel found in the five channels immediately preceding the peak and five channels immediately following the peak. This is subtracted from the area under the peak.
4. Assume that peaks are a Gaussian distribution. Thus, $FWHM = 2.354\sigma$

After completely analyzing the data, it was necessary to develop another sorting program which allows me to gate in two dimensions: 2D GATE. These three new programs are listed in the appendix.

2. Results and Discussion

Figs. 3-4 and 3-5 show the correlation between the centroid of the 1332.5-keV γ -ray peak and two TAC's: the 0.7 and 0.5 fractions. On the 0.5 fraction axis the interval between each line is about 1.5 nsec. On the 0.7 fraction axis, it is 3.3 nsec. The centroid axis is 39 channels from the bottom to the top (on a log scale). Fig. 3-5 was obtained by rotating fig. 3-4 by 90° clockwise about the centroid axis. The relative yield for each 1332.5-keV peak versus the two TAC settings is shown in figs. 3-6 and 3-7. Again, Fig. 3-7 was obtained by a similar rotation of fig. 3-6.

As can be seen in figs. 3-6 and 3-7, the observed events are not

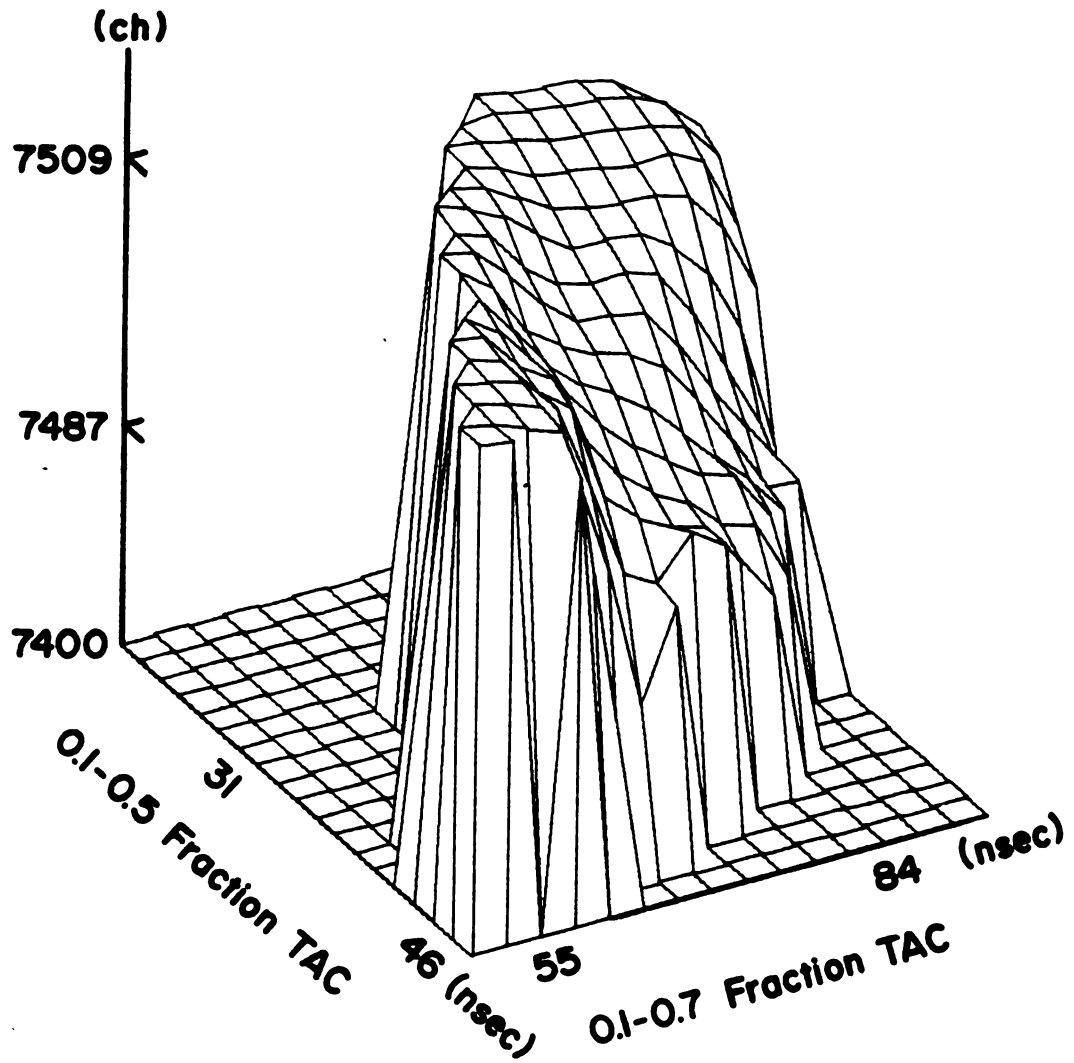


Figure 3-4

The correlation between the centroid of the 1332.5-keV peak and the two TAC signals.

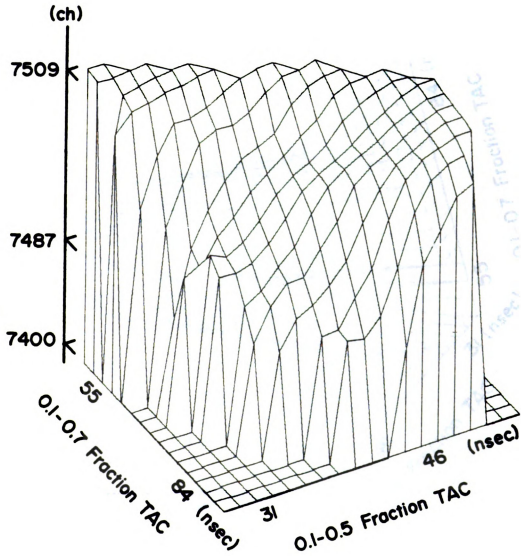


Figure 3-5

90° clockwise rotation of fig. 3-4.

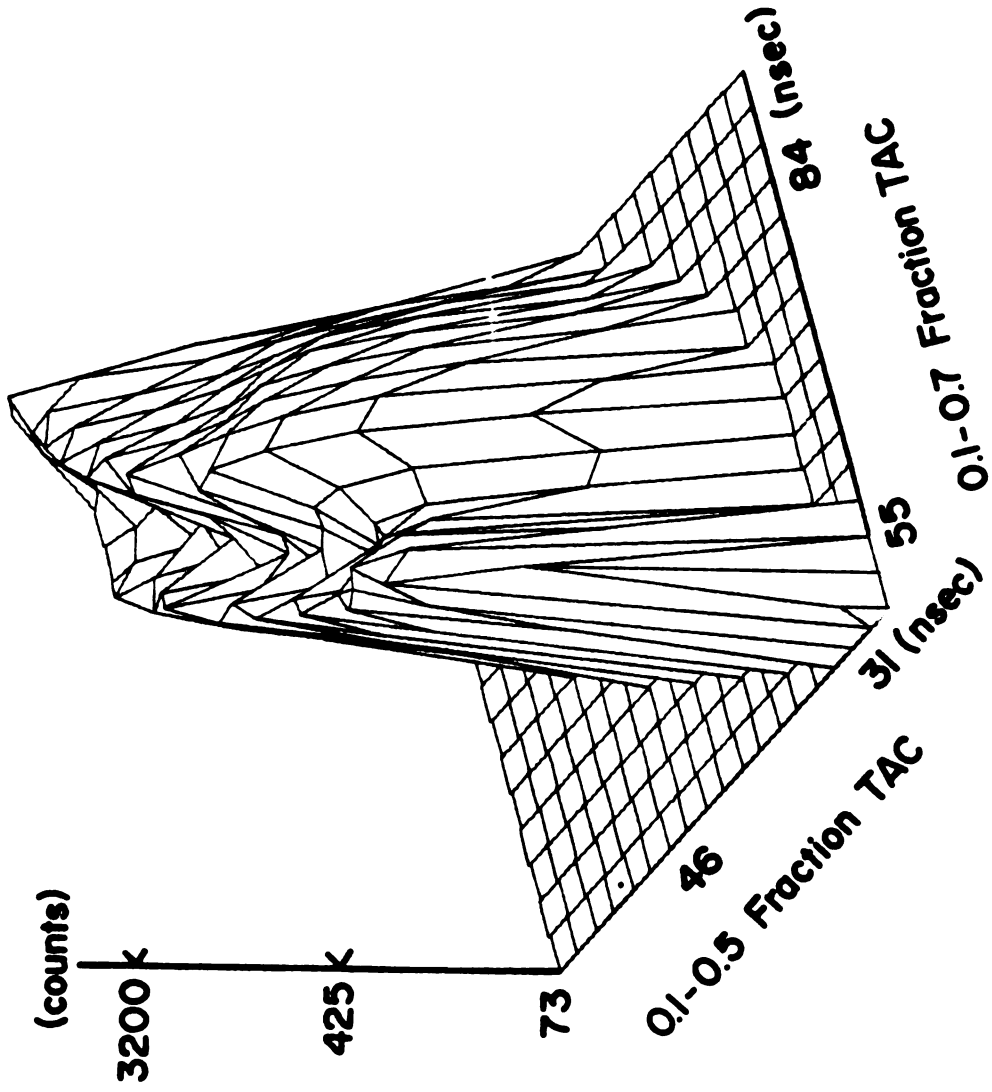


Figure 3-6

The relative yield for each 1332.5-keV peak vs the two TAC signals.

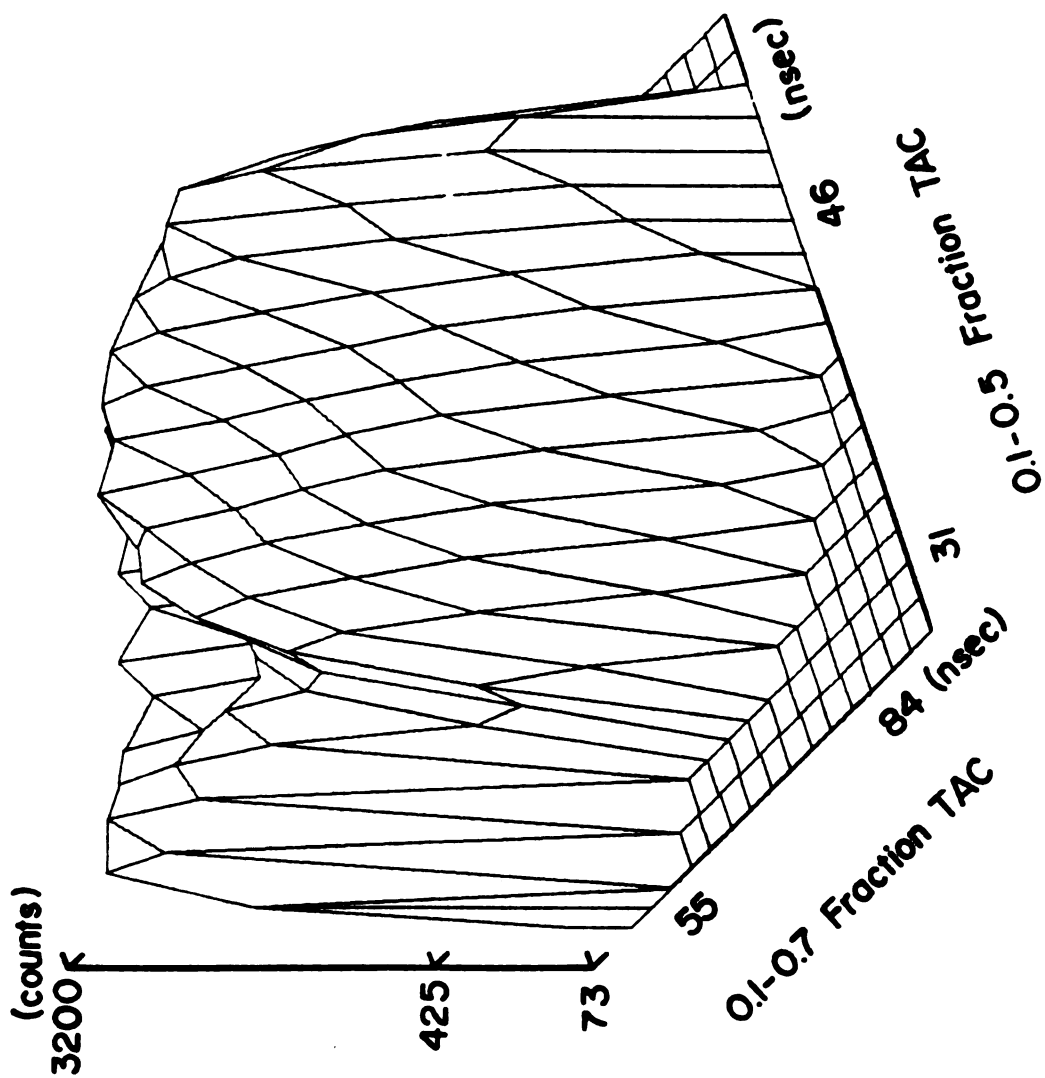
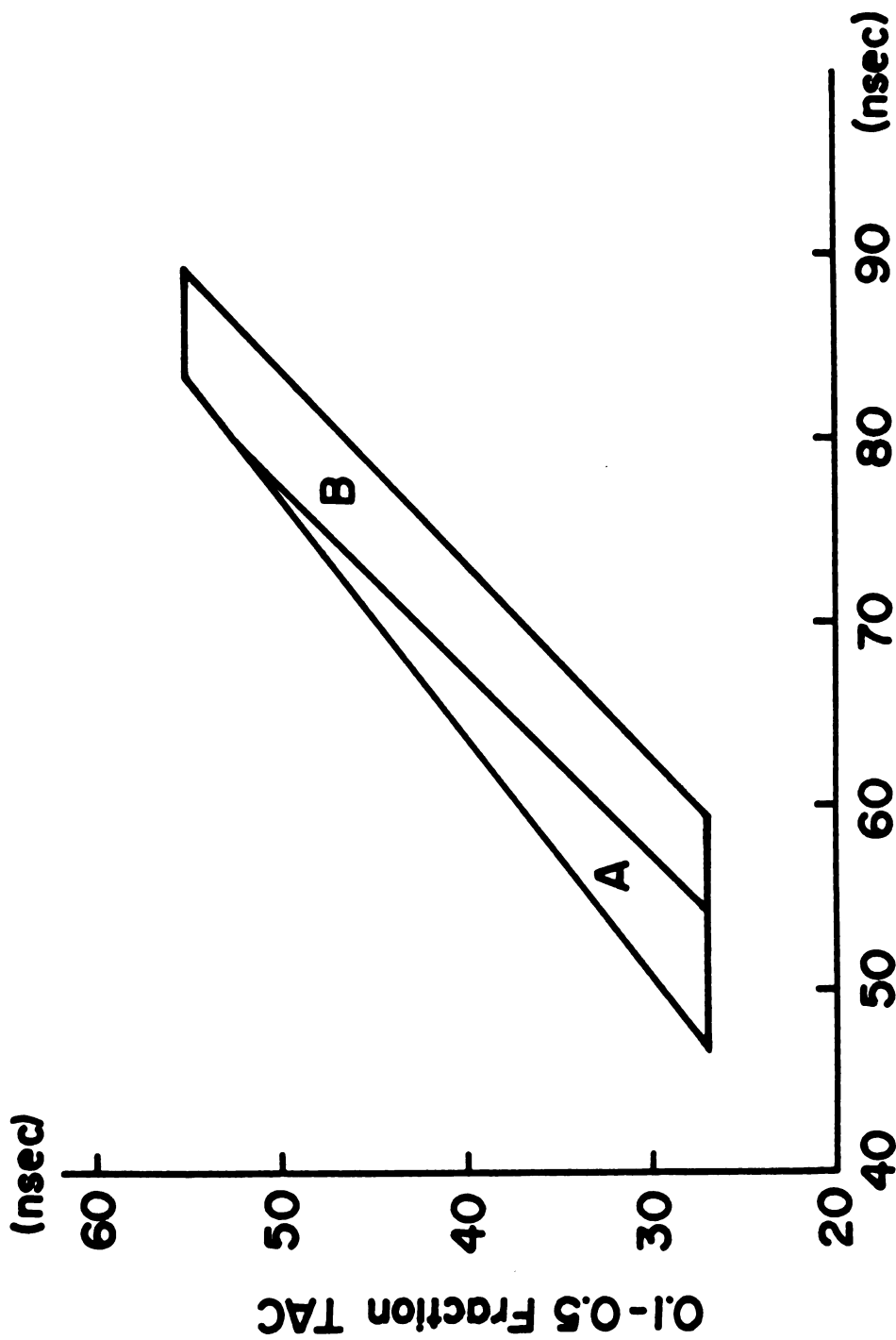


Figure 3-7

90° clockwise rotation of fig. 3-6.

distributed on a line, but rather in a broad area. The centroid versus the rise-time, figs. 3-4 and 3-5, show that the higher yield areas of figs. 3-6 and 3-7 also have higher centroids. This result agrees with my predictions: These lower yield and centroid regions result from the neutron-damaged pulses and the higher yield and centroid regions, from undamaged pulses.

The energy resolution in the non-neutron damaged area is about 2.59 keV FWHM and in the neutron damaged area about 3 keV. After accumulating events from the non-neutron area (A in fig. 3-8) by 2D GATE program, we are able to improve the energy resolution to 2.61 keV (at 1332.5 keV) with 10% efficiency, corresponding to a 46% improvement in energy resolution. With 28% efficiency in the gated area A and B in fig. 3-8, we get 2.96 keV energy resolution, 40% improvement in energy resolution. The spectrum resulting from area A in fig. 3-8 is shown in fig. 3-9 with the original spectrum for comparison, and I have blown up a portion of fig. 3-9 in fig. 3-10. Since each individual gated energy resolution is much better than the raw data, in principle it is possible to make the pulse-height correction for a coaxial detector by finding a pulse-height function which is a function of both the rise-time 0.1-0.5 and 0.1-0.7 fractions.



0.1-0.7 Fraction TAC

Figure 3-8

The two dimensional plots displaying the gated regions for 2D GATE.

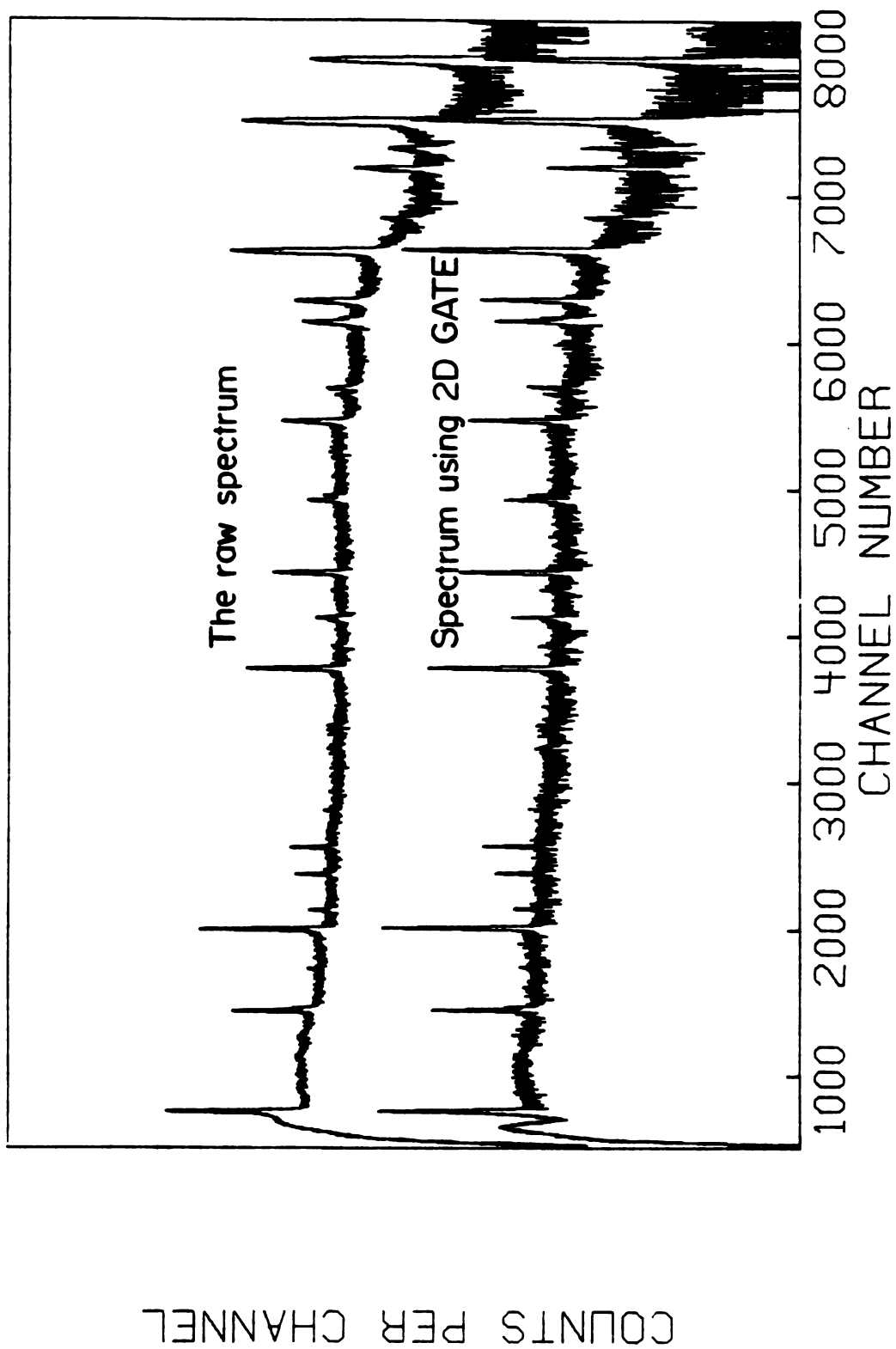


Figure 3-9 .

Spectrum with the 2D GATE (bottom) compared with the raw data (top).

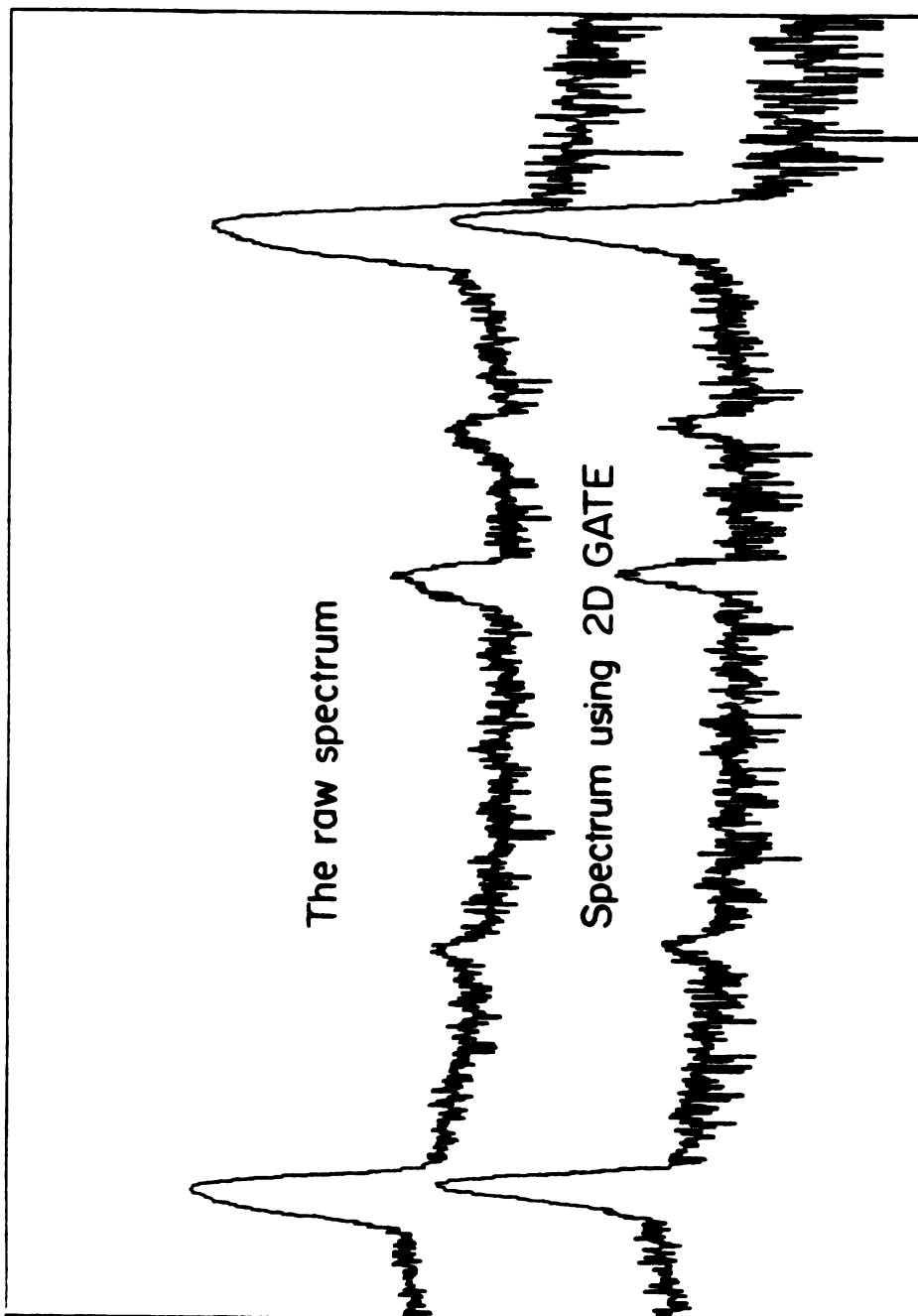


Figure 2-10

Blow up of a portion of fig. 3-9

CHAPTER IV
CONCLUSIONS

It is evident from these results that neutron damage changes the normal pulse-heights, and these different pulse-height signals result in lower overall energy resolution. It is also possible to correct for this effect and improve the overall energy resolution. When the energy resolution of individual rise-time gated spectrum slices is better than the composite "all-events" spectrum, one can significantly improve the resolution of overall spectrum by either employing the pulse-height correction method or collecting data only from non-neutron damaged areas. By using the pulse-height correction method, the improvement in energy resolution can be obtained without an appreciable loss in efficiency. In other words, one can salvage the "degraded" spectrum parts, slice by slice, by shifting them to their undegraded equivalent and then adding them up to obtain an improved spectrum.

For a coaxial detector, it is necessary to use two different rise-time discriminators because of its more complicated structure. Also, it may be possible to apply the pulse-height correction to this type of detector by finding the function,

$$Ch_{\text{shift}} = \beta f(t_1, t_2) \quad (4)$$

Here β is energy dependent constant, and $f(t_1, t_2)$ is a function of the two rise-times. The energy dependent constant can be obtained by

investigating the peak centroids versus the energy relationship as described in chapter 2.

Finally, this phenomenon should be studied using gaseous proportional counters, where conditions can be controlled more readily. We may ultimately discover that the sequence of events for collection of charge carriers within the detector producing a pulse, particularly a photopeak pulse, from a Ge(Li) detector are considerably more complex than we had realized. In the meantime, using fast pulse rise-time discrimination technique can be a practical way for significantly improving the quality of γ -ray spectra.

BIBLIOGRAPHY

BIBLIOGRAPHY

- [Au72] II-Event, written for the MSU NSCL Sigma-7 computer by R. Au (1972).
- [Au75] II-Event Recover, written for the MSU NSCL Sigma-7 computer by R. Au (1975).
- [Au67] R. L. Auole, D. B. Berry, G. Berzins, L. M. Beyer, R. C. Etherton, W. H. Kelly, and Wm. C. McHarris,, Nucl. Instr. and Meth. 51 (1967) 61.
- [Ba74] R. Baader, W. Patzner, and H. Wohlfarth, Nucl. Instr. and Meth. 117 (1974) 609.
- [Be77] R. Beetz, W. L. Posthumus, F. W. N. Deboer, J. L. Maarleveld, A. Van der Schaaf, and J. Konijn, Nucl. Instr. and Meth. 144 (1977) 353.
- [Be72] D. Belusa, E. Fretwurst, F. Jaber, and G. Lindstrom, Nucl. Instr. and Meth. 101 (1972) 171.
- [Co71] B. L. Cohen, "Experimental Methods of Nuclear Physics", Chap. 9 in Concepts of Nuclear Physics, McGraw-Hill, 1971.
- [Gi71] See, e.g., G. C. Giesler, Wm. C. McHarris, R. A. Warner, and W. H. Kelly, Nucl. Instr. and Meth. 91 (1971) 313.
- [Go74] F. S. Goulding and R. H. Pehl, "Semiconductor Radiation Detectors", Chap. III.A in Nuclear Spectroscopy and Reactions, Ed. by J. Cerny, Academic Press, 1974.

- [Ie71] "An American National IEEE Standard Test Procedure for Germanium Gamma-Ray Detectors", ANSI IEEE N42.8-1972 Std. 325-1971.
- [Ka80] Private communication with J. Kasagi.
- [Kr68] H. W. Kraner, C. Chasman, and K. W. Jones, Nucl. Instr. and Meth 62 (1968) 173.
- [Li74] G. Lindstrom and R. Lisclat, Nucl. Instr. and Meth. 116 (1974) 181.
- [Ma68] J. W. Mayer, "Search for Semiconductor Materials for Gamma-Ray Spectroscopy", Chap. 5 in Semiconductor Detectors, Ed. G. Bertoloni and A. Coche, Wiley (1968).
- [Pe72] Eg., R. H. Pehl, R. C. Cordi, and F. S. Goulding IEEE Trans. Nucl. Sci. NS-19, No. 1 (1972) 265.
- [Wh79] A summary of the present state of the art with respect to certain "exotic" detector materials is given by R. C. Whited and M. M. Schieber, Nucl. Instr. and Meth. 162 (1979) 113.

APPENDICES

APPENDIX

A. Event Rec

```

1.      DIMENSION IDATA1(200,25,10),IDATA2(200,25,10),IDI1(50000),ISEQ(4)
2.      +,IDI2(50000),ITITLE(20),IARRY(4),JTITLE(20)
3.      EQUIVALENCE(IDATA1(1,1,1),IDI1(1))
4.      EQUIVALENCE(IDATA2(1,1,1),IDI2(1))
5.      READ(105,10)ITC1,MAX1,ICF1
6.      READ(105,10)ITC2,MAX2,ICF2
7.      READ(105,10)IENG,MAX3,ICF3
8.      READ(105,15)MTSTOP
9.      READ(105,100)JTITLE
10.     10      FORMAT(3I)
11.     15      FORMAT(1I)
12.     READ(105,20)ITYPE,NUM
13.     20      FORMAT(2I)
14.     ISEQ(1)=0
15.     ISEQ(2)=1
16.     ISEQ(3)=3
17.     WRITE(100,25)ITC1,MAX1,ICF1
18.     WRITE(100,25)ITC2,MAX2,ICF2
19.     WRITE(100,26)IENG,MAX3,ICF3
20.     25      FORMAT(1H0,'TAC',15,5X,'MAX',15,5X,'ICF',15)
21.     OUTPUT ITYPE,NUM,ISEQ
22.     26      FORMAT(1H0,'ENG',15,5X,'MAX',15,5X,'ICF',15)
23.     DO 17 J=1,50000
24.     IDI2(J)=0
25.     IDI1(J)=0
26.     CALL EUSET(110,ITYPE,NUM,ITITLE,M,ISEQ)
27.     IF(M.EQ.0)GO TO 50
28.     IF(M.EQ.1)GO TO 450
29.     IF(M.EQ.2)GO TO 451
30.     IF(M.EQ.3)GO TO 452
31.     450     WRITE(100,150)
32.     GO TO 999
33.     150     FORMAT(1H0,'TAPE READ ERROR')
34.     GO TO 999
35.     451     WRITE(100,151)
36.     151     FORMAT(1H0,'PARAMETER ERROR')
37.     GO TO 999
38.     452     WRITE(100,152)
39.     152     FORMAT(1H0,'ILLEGL REQUEST AT SET')
40.     GO TO 999
41.     50      WRITE(100,500)ITITLE
42.     500     FORMAT(1H0,'TITLE',5X,20A4)
43.     ICOIN1=0
44.     ICOIN2=0
45.     IEVENT=0
46.     JREO=0
47.     JADCE=0
48.     ILEG=0
49.     301     IF(MTSTOP.LE.0)GO TO 310
50.     IF(IEVENT.EQ.MTSTOP) GO TO 400
51.     310     IEVENT=IEVENT+1
52.     CALL EUGET(IARRY,N)
53.     IF(N.EQ.0)GO TO 200
54.     IF(N.EQ.-1)GO TO 400
55.     IF(N.EQ.1)GO TO 260
56.     IF(N.EQ.2)GO TO 410
57.     IF(N.EQ.3)GO TO 420
58.     200     IF(IARRY(1).LT.ITC1.OR.IARRY(1).GT.MAX1)GO TO 301
59.     IF(IARRY(3).LT.ITC2.OR.IARRY(3).GT.MAX2)GO TO 301
60.     IF(IARRY(2).LT.IENG.OR.IARRY(2).GT.MAX3) GO TO 301
61.     K=(IARRY(1)-ITC1)/ICF1+1
62.     J=(IARRY(3)-ITC2)/ICF2+1
63.     I=(IARRY(2)-IENG)/ICF3+1
64.     IF(K.GT.20) GO TO 301
65.     IF(J.GT.25) GO TO 301
66.     IF(I.GT.200)GO TO 301
67.     IF(K.GE.11) GO TO 250
68.     IDATA1(I,J,K)=IDATA1(I,J,K)+1
69.     ICOIN1=ICOIN1+1
70.     GO TO 301
71.     250     K=K-10
72.     IDATA2(I,J,K)=IDATA2(I,J,K)+1
73.     ICOIN2=ICOIN2+1
74.     GO TO 301
75.     260     JREO=JREO+1
76.     GO TO 301
77.     410     JADCE=JADCE+1
78.     GO TO 301

```

```

79. 420 ILEG=ILEG+1
80. GO TO 301
81. 400 WRITE(200,100)JTITLE
82. WRITE(201,100)JTITLE
83. OUTPUT ICOIN1,ICOIN2
84. WRITE(202,100)JTITLE
85. WRITE(203,100)JTITLE
86. WRITE(204,100)JTITLE
87. WRITE(205,100)JTITLE
88. WRITE(206,100)JTITLE
89. WRITE(207,100)JTITLE
90. 100 FORMAT(20A4)
91. CALL CPUNCH(IDI1(1),16200,1,NERR,0,200)
92. CALL CPUNCH(IDI1(16201),16200,2,NERR,0,201)
93. CALL CPUNCH(IDI1(32401),16200,3,NERR,0,202)
94. CALL CPUNCH(IDI1(48601),1400,4,NERR,0,203)
95. CALL CPUNCH(IDI2(1),16200,5,NERR,0,204)
96. CALL CPUNCH(IDI2(16201),16200,6,NERR,0,205)
97. CALL CPUNCH(IDI2(32401),16200,7,NERR,0,206)
98. CALL CPUNCH(IDI2(48601),1400,8,NERR,0,207)
99. WRITE(100,700) JREO
100. 700 FORMAT(1H0,'ERROR ON READ OPERATION',2X,I8)
101. WRITE(100,701) JADCE
102. 701 FORMAT(1H0,'ADC GROUP ERROR',2X,I8)
103. OUTPUT IEVENT
104. 999 STOP
105. END

```

B. Auto Cen

```

1.      DIMENSION ITIT(16),IFNAM(10),IDT(16384),Y(16384),ATIT(20)
2.      INTEGER Y
3.      READ(105,50) ATIT
4.      50  FORMAT(20A4)
5.      15  READ(105,21,END=900),((IFNAM(I),I=2,10)
6.      DO 5 I=1,16384
7.      IDT(I)=0
8.      Y(I)=0
9.      5   CONTINUE
10.     21  FORMAT(9A4)
11.     READ(105,25) ISTART, ISTOP, KCHAN
12.     25  FORMAT(3I)
13.     READ(105,26) INTER
14.     26  FORMAT(1I)
15.     WRITE(100,500),((IFNAM(I),I=2,10)
16.     500  FORMAT(1H0,16A4)
17.     IFNAM(1)=20
18.     CALL UNLOAD(110)
19.     CALL ASSIGN(110,1,IFNAM,0)
20.     READ(110,30,END=15) ITIT
21.     30  FORMAT(16X,16A4)
22.     505  FORMAT(1H0,'START CHIS ',I5,10X,'STOP CH IS ',I5,10X,'THIS IS A PE
23.     +AK STARTING AT THE ',I5)
24.     CALL CREAD(IDT,NCHAN,NRUN,NREE,NSTART,110)
25.     WRITE(100,505) ISTART, ISTOP, KCHAN
26.     WRITE(100,27) INTER
27.     27  FORMAT(1H0,'INTERVAL IS ',I5)
28.     IF(NREE.NE.0) GO TO 800
29.     CALL SMOOTH(Y, IDT, ISTART, ISTOP)
30.     WRITE(106,50) ATIT
31.     CALL CPUNCH(Y,16200,001,NERR,0,106)
32.     C
33.     C
34.     C
35.     IK=INTER
36.     IA=200
37.     IB=0
38.     ISTART=ISTART+40
39.     DO 100 I=ISTART,ISTOP
40.     ICHAN=0
41.     IHICOUNT=-1
42.     DO 110 J=ISTART,IA
43.     IF(IHICOUNT.GT.Y(J)) GO TO 110
44.     IHICOUNT=Y(J)
45.     ICHAN=J
46.     110  CONTINUE
47.     IF(IHICOUNT.LT.1) GO TO 150
48.     K=ICHAN
49.     IPL=K-IK
50.     IPR=K+IK
51.     SLB=(IDT(K-IK-1)+IDT(K-IK-2)+IDT(K-IK-3)+IDT(K-IK-4)+IDT(K-IK-5))/
52.     +5
53.     SRB=(IDT(K+IK+1)+IDT(K+IK+2)+IDT(K+IK+3)+IDT(K+IK+4)+IDT(K+IK+5))/
54.     +5.
55.     C
56.     C
57.     C
58.     SR=IPR
59.     SL=IPL
60.     BACKG=0
61.     CEN=0.
62.     SBACK=0.
63.     AREA=0.
64.     DCEN=0.
65.     N=-1
66.     FK=(SRB-SLB)/(SR-SL)
67.     DO 160 II=IPL,IPR
68.     N=N+1
69.     BACKG=SLB+FK*(FLOAT(N))
70.     A=IDT(II)-BACKG
71.     AREA=AREA+A
72.     CEN=A*II+CEN
73.     SBACK=SBACK+BACKG
74.     160  CONTINUE
75.     ERR=SQRT(2.*SBACK+AREA)
76.     CEN=CEN/AREA
77.     DO 170 JK=IPL,IPR
78.     170  DCEN=DCEN+(FLOAT(JK)-CEN)**2*(IDT(JK)+BACKG)

```

```

79.      DCEN=SQRT(DCEN)/AREA
80.      C
81.      C
82.      C
83.      N=-1
84.      SA=0
85.      SB=0
86.      SUMB=0
87.      SUMA=0
88.      BACK=0
89.      FE=0
90.      DO 200 MM=IPL, IPR
91.      N=N+1
92.      BACK=SLB+FK*(FLOAT(N))
93.      AS=IDT(MM)-BACK
94.      AA=((MM-CEN)**2)*AS
95.      BB=((MM-CEN+DCEN)**2)*AS
96.      SUMA=SUMA+AA
97.      SUMB=SUMB+BB
98.      200 CONTINUE
99.      OUTPUT SUMA, SUMB, AREA
100.     SA=2.354*SQRT(SUMA/(AREA-1))
101.     SB=2.354*SQRT(SUMB/(AREA-1))
102.     FE=SB-SA
103.     SCHAN=KCHAN+(CEN-IB*200)
104.     YCHAN=KCHAN+((CEN-DCEN)-IB*200)
105.     ZCHAN=KCHAN+(CEN+DCEN)-IB*200)
106.     WRITE(100,605)
107.     605 FORMAT(1H0,3X,'PL',6X,'PR',6X,'SLB',6X,'SRB',6X,'AREA',6X,'ERR',6X
108.     +,'SBACK',6X,'CEN',6X,'DCEN',6X,'FWHM',6X,'DFW',6X,'CHAN',6X,'LCHAN'
109.     +,6X,'MCHAN')
110.     WRITE(100,610)IPL,IPR,SLB,SLR,AREA,ERR,SBACK,CEN,DCEN,SA,FE,SCHAN,
111.     +YCHAN,ZCHAN
112.     610 FORMAT(1H0,X,I5,2X,I5,2X,F5.2,2X,F5.2,3X,F10.3,3X,F5.4,3X,F10.3,3X
113.     +,F10.4,1X,F7.4,2X,F7.3,2X,F6.4,2X,F8.3,2X,F9.4,2X,F9.4)
114.     150 CONTINUE
115.     IB=IB+1
116.     ISTART=IB*200
117.     IA=ISTART+200
118.     ISTART=ISTART+50
119.     IF(ISTART.GE.ISTOP) GO TO 15
120.     CONTINUE
121.     800 WRITE(100,550)NREE
122.     550 FORMAT(1H0,I2)
123.     GO TO 900
124.     900 STOP
125.     END

1.      C
2.      SUBROUTINE SMOOTH(Y, IDT, ISTART, ISTOP)
3.      C
4.      DIMENSION Y(1), IDT(1)
5.      INTEGER Y
6.      YI=IDT(ISTART)
7.      IST=ISTOP-1
8.      IS=0
9.      DO 99 I=ISTART, ISTOP
10.     IS=IS+IDT(I)
11.     WRITE(100,100)IS
12.     100 FORMAT(1H0,I6)
13.     DO 10 I=ISTART, IST
14.     10 Y(I)=(IDT(I-1)+2.0*IDT(I)+IDT(I+1))/4.0
15.     RETURN
16.     END

```

C. 2D GATE

```

1.   DIMENSION IGM1(1024), IGM2(1024), IGM3(1024), IGMX1(1024), ISEQ(3),
2.   +IGMX2(1024), IGMX3(1024), IDATA1(8192), IDATA2(8192), IDATA3(8192), IAR
3.   +RY(3), ITITLE(20), JTITLE(20)
4.   REAL IDXMIN, IDYM, IDMX, IDXMIN2, IDYM2, IDMX2, IDXMIN3, IDYM3, IDMX3
5.   DO 50 I=1, 1024
6.     IGMX1(I)=0
7.     IGMX2(I)=0
8.     IGMX3(I)=0
9.     IGM1(I)=1000
10.    IGM2(I)=1000
11.    IGM3(I)=1000
12.    DO 55 I=1, 8192
13.      IDATA1(I)=0
14.      IDATA2(I)=0
15.      IDATA3(I)=0
16.    READ(105, 105) JTITLE
17.    WRITE(100, 106) JTITLE
18.    FORMAT(1H0, 20A4)
19.    READ(105, 15) MTSTOP
20.    FORMAT(1I)
21.    READ(105, 20) ITC1, IMAX1, ITC2, IMAX2, ITC3, IMAX3
22.    FORMAT(6I)
23.    WRITE(100, 16) ITC1, IMAX1, ITC2, IMAX2, ITC3, IMAX3
24.    FORMAT(1H0, 'TAC1', I5, 5X, 'TAC MAX1', I4, 9X, 'TAC2', I5, 5X, 'TAC MAX2',
25.    +I5, 9X, 'TAC3', I5, 5X, 'TAC MAX3', I5)
26.    READ(105, 26) IX1, IX2, IX3, IX4, IY1, IX21, IX22, IX23, IX24, IY2, IX31, IX32,
27.    +IX33, IX34, IY3
28.    FORMAT(15I)
29.    WRITE(100, 25) IX1, IX2, IX3, IX4, IY1
30.    FORMAT(1H0, '1ST GATE---', 'X1--', I4, 3X, 'X2--', I4, 3X, 'X3--', I4, 3X, 'X4
31.    +---', I4, 3X, 'Y1--', I4)
32.    WRITE(100, 27) IX21, IX22, IX23, IX24, IY2
33.    FORMAT(1H0, '2ND GATE---', 'X1--', I4, 3X, 'X2--', I4, 3X, 'X3--', I4, 3X, 'X4
34.    +---', I4, 3X, 'Y1--', I4)
35.    WRITE(100, 28) IX31, IX32, IX33, IX34, IY3
36.    FORMAT(1H0, '3RD GATE---', 'X1--', I4, 3X, 'X2--', I4, 3X, 'X3--', I4, 3X, 'X4
37.    +---', I4, 3X, 'Y1--', I4)
38.    IDXMIN=IX1-IX2
39.    IDYM=ITC1-IMAX1
40.    IDMX=IX3-IX4
41.    SLOPMI=IDYM/IDXMIN
42.    SLOPMX=IDYM/IDMX
43.    OUTPUT SLOPMI, SLOPMX
44.    DO 100 I=ITC1, IMAX1
45.      IGMX1(I)=I/SLOPMX-IY1/SLOPMX+IX3
46.      IGM1(I)=I/SLOPMI-IY1/SLOPMI+IX1
47.      IDXMIN2=IX21-IX22
48.      IDYM2=ITC2-IMAX2
49.      IDMX2=IX23-IX24
50.      SLOPMI2=IDYM2/IDXMIN2
51.      SLOPMX2=IDYM2/IDMX2
52.      OUTPUT SLOPMI2, SLOPMX2
53.      DO 101 J=ITC2, IMAX2
54.        IGMX2(J)=J/SLOPMX2-IY2/SLOPMX2+IX23
55.        IGM2(J)=J/SLOPMI2-IY2/SLOPMI2+IX21
56.        IDXMIN3=IX31-IX32
57.        IDYM3=ITC3-IMAX3
58.        IDMX3=IX33-IX34
59.        SLOPMI3=IDYM3/IDXMIN3
60.        SLOPMX3=IDYM3/IDMX3
61.        OUTPUT SLOPMI3, SLOPMX3
62.        DO 102 K=ITC3, IMAX3
63.          IGMX3(K)=K/SLOPMX3-IY3/SLOPMX3+IX33
64.          IGM3(K)=K/SLOPMI3-IY3/SLOPMI3+IX31
65.        WRITE(100, 600) IGMX1
66.        WRITE(100, 600) IGM1
67.        WRITE(100, 600) IGMX2
68.        WRITE(100, 600) IGM2
69.        WRITE(100, 600) IGMX3
70.        WRITE(100, 600) IGM3
71.      FORMAT(1H0, 20I5)
72.    NUM=3
73.    ISEQ(1)=0
74.    ISEQ(2)=1
75.    ISEQ(3)=3
76.    CALL EUSER(110, ITYPE, NUM, ITITLE, M, ISEQ)
77.    IF(M.EQ.0)GO TO 51
78.    IF(M.EQ.1)GO TO 450

```

```

79.      IF(M.EQ.2)GO TO 451
80.      IF(M.EQ.3)GO TO 452
81.      450  WRITE(100,150)
82.      GO TO 999
83.      150  FORMAT(1H0,'TAPE READ ERROR')
84.      GO TO 999
85.      451  WRITE(100,151)
86.      151  FORMAT(1H0,'PARAMETER ERROR')
87.      GO TO 999
88.      452  WRITE(100,152)
89.      152  FORMAT(1H0,'ILLEGL REQUEST AT SET')
90.      GO TO 999
91.      51   WRITE(100,500)ITITLE
92.      500  FORMAT(1H0,'TITLE',5X,20A4)
93.      ICOIN1=0
94.      ICOIN2=0
95.      ICOIN3=0
96.      IEVENT=0
97.      JREQ=0
98.      JADCE=0
99.      ILEG=0
100.     301  IF(MTSTOP.LE.0)GO TO 310
101.     IF(IEVENT.EQ.MTSTOP) GO TO 400
102.     310  IEVENT=IEVENT+1
103.     CALL EUGET(IARRY,N)
104.     ICH7=IARRY(1)
105.     ICHE=IARRY(2)
106.     ICH5=IARRY(3)
107.     IF(N.EQ.0)GO TO 200
108.     IF(N.EQ.-1)GO TO 400
109.     IF(N.EQ.1)GO TO 260
110.     IF(N.EQ.2)GO TO 410
111.     IF(N.EQ.3)GO TO 420
112.     200  IF(ICH7.LT.IGMI1(ICHS).OR.ICH7.GT.IGMX1(ICHS))GO TO 350
113.     IDATA1(ICHE)=IDATA1(ICHE)+1
114.     ICOIN1=ICOIN1+1
115.     350  IF(ICH7.LT.IGMI2(ICHS).OR.ICH7.GT.IGMX2(ICHS))GO TO 351
116.     IDATA2(ICHE)=IDATA2(ICHE)+1
117.     ICOIN2=ICOIN2+1
118.     351  IF(ICH7.LT.IGMI3(ICHS).OR.ICH7.GT.IGMX3(ICHS))GO TO 301
119.     IDATA3(ICHE)=IDATA3(ICHE)+1
120.     ICOIN3=ICOIN3+1
121.     GO TO 301
122.     260  JREQ=JREQ+1
123.     GO TO 301
124.     410  JADCE=JADCE+1
125.     GO TO 301
126.     420  ILEG=ILEG+1
127.     GO TO 301
128.     400  WRITE(201,105)JTITLE
129.     WRITE(202,105)JTITLE
130.     WRITE(203,105)JTITLE
131.     105  FORMAT(20A4)
132.     CALL CPUNCH(IDATA1,8192,1,NERR,0,201)
133.     CALL CPUNCH(IDATA2,8192,2,NERR,0,202)
134.     CALL CPUNCH(IDATA3,8192,3,NERR,0,203)
135.     WRITE(100,700) JREQ
136.     700  FORMAT(1H0,'ERROR ON READ OPERATION',2X,I8)
137.     WRITE(100,701) JADCE
138.     701  FORMAT(1H0,'ADC GROUP ERROR',2X,I8)
139.     OUTPUT IEVENT
140.     OUTPUT ICOIN1,ICOIN2,ICOIN3
141.     999  STOP
142.     END

```

MICHIGAN STATE UNIVERSITY LIBRARIES



3 1293 03145 2349